**Suppl. Fig. 1 (Related to Main Figure 1). Role of RN to dorsal CA1 projecting cells in contextual memory linking**

A. Exploration of a novel context increased cFos expression in 5HT+ positive cells of RN (unpaired t-test, n=5, **p<0.01) Example images. Scale bar, 50µm. 5HT- magenta, cFos- cyan.

B. Schematics of experimental design. Example images. DAPI- blue. Scale bar, 100µm.

C. Schematics of experimental design. Context A- Ctx A, Context B- Ctx B, Context C- Ctx C (neutral). CNO was given to all mice. Inhibition of RN cells projecting to dCA1 during exploration of context A did not affect the process of memory linking. (Control, n=10; LC inhibited, n=9. Two-way repeated measures ANOVA, Sidak post hoc. *p <0.05, ****p<0.0001)

D. Schematics of the experimental procedure. Inhibition of RN cells projecting to dCA1 during exploration of a novel context significantly reduced cFos expression in the mcherry positive cells of RN (unpaired t-test, n=4, ****p<0.0001).
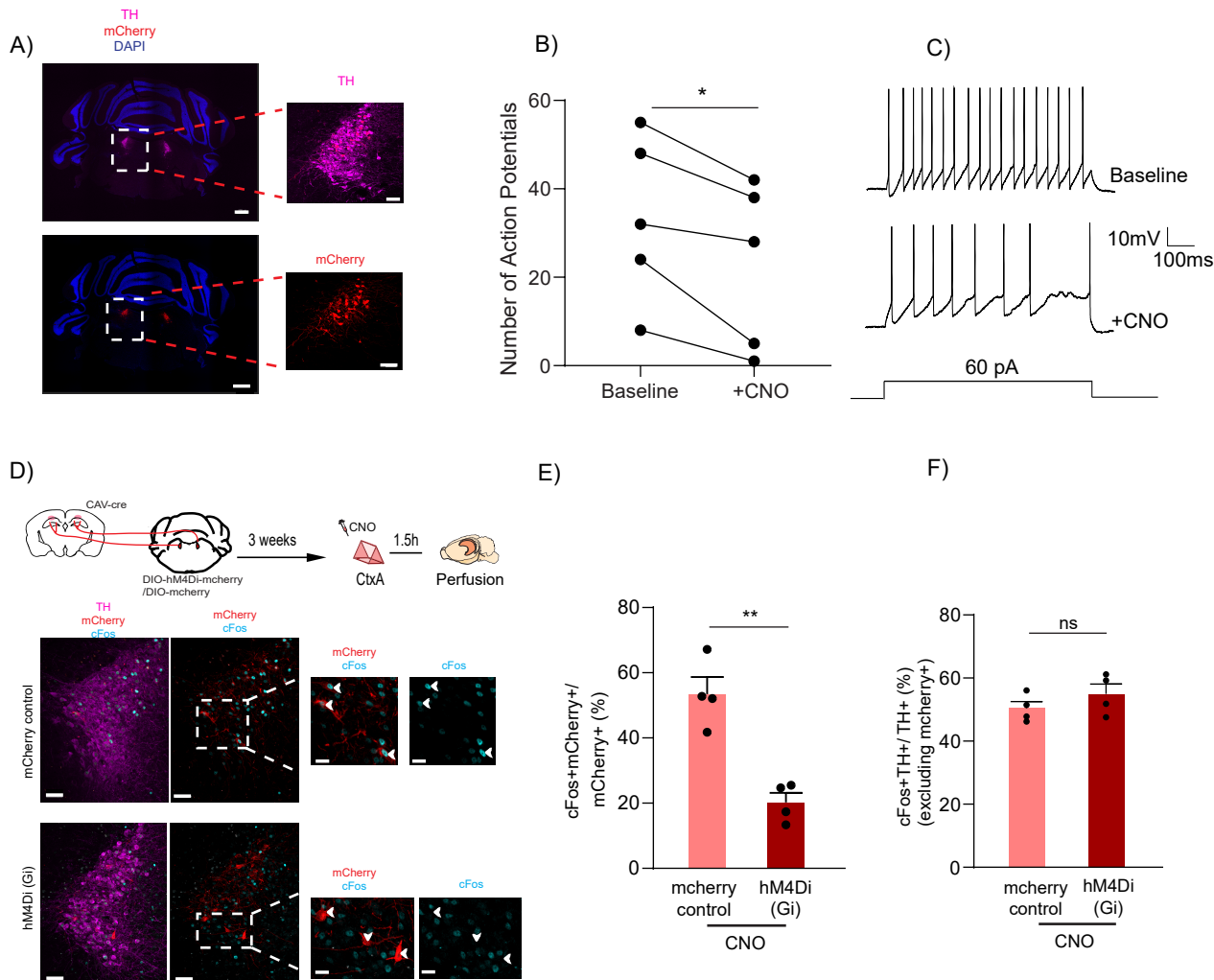
Suppl. Fig 2 (Related to Main Figures 1 and 3). Effect of activation of hM4Di receptors on firing rate of LC neurons and the cFos expression triggered by contextual exploration.

A. Representative images for injection sites at LC. TH- magenta, mCherry- red, DAPI- blue. Scale bar, 300μm.

B. Bath application of CNO reduces the number of action potentials fired by LC neurons compared to baseline.Paired t-test, *p<0.05. n=5

C.Representative traces showing firing responses to a 60pA current injection in LC neurons.

D. Schematics of the experimental procedure. Example images. TH- magenta, mCherry- red, cFos- cyan. Scale bar, 50μm.

E. Inhibition of LC cells projecting to dCA1 during exploration of a novel context significantly reduced cFos expression in the mcherry positive cells of LC (unpaired t-test, n=4, **p<0.01).

F. Inhibition of LC cells projecting to dCA1 during exploration of a novel context did not affect cFos expression in the TH positive cells (excluding mcherry) of LC (unpaired t-test, n=4, ns p>0.05).
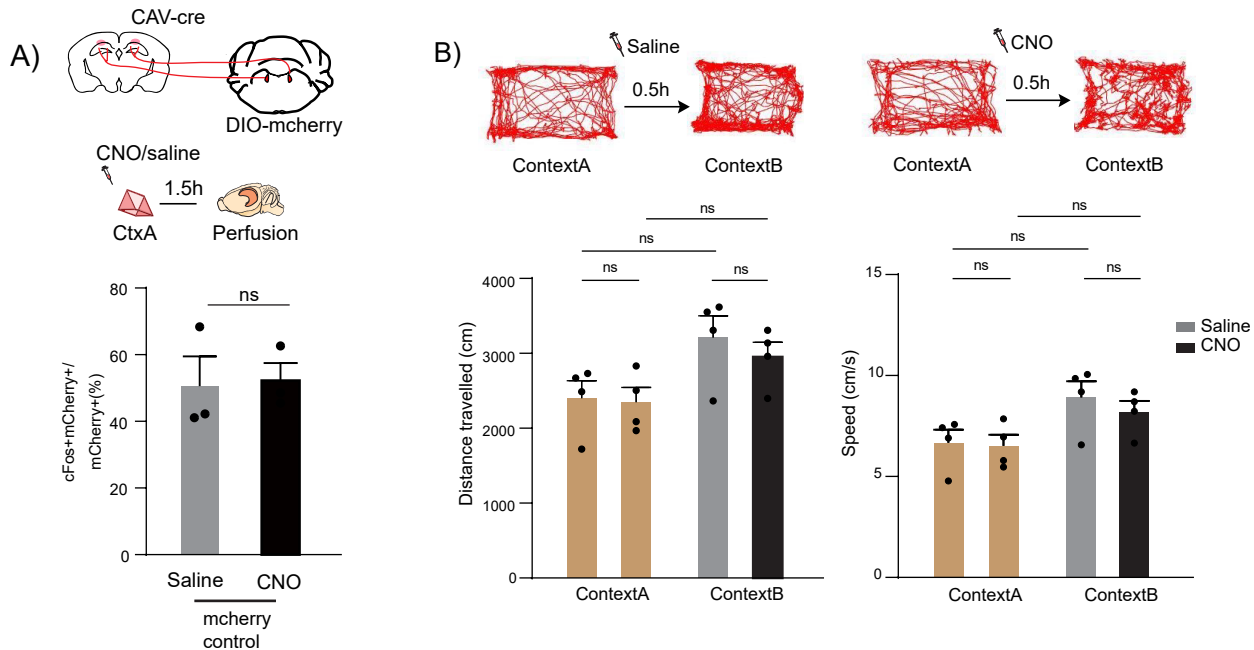
Suppl. Fig 3 (Related to Main Figures 1, 2, 4 and 7). Effect of CNO on cFos expression and exploratory behavior of mice.

A. Schematics of the experimental procedure. Administration of saline or CNO 30min before exploration of a novel context did not affect cFos expression in the mcherry-positive cells of LC (unpaired t-test, n=3, n sp>0.05).

B. The mice were allowed to explore a novel context A. Then immediately, one group was injected with saline and another with CNO. 30min later, they were taken to another novel context B for exploration. Sample traces. The distance travelled and the speed of movement showed that all the mice were equivalent before any treatment (context A; beige-no drug). Furthermore, there was no difference between the groups after the treatment (context B, grey-Saline, black-CNO). n=4, two-way RM ANOVA, Sidak post hoc. ns p> 0.05.
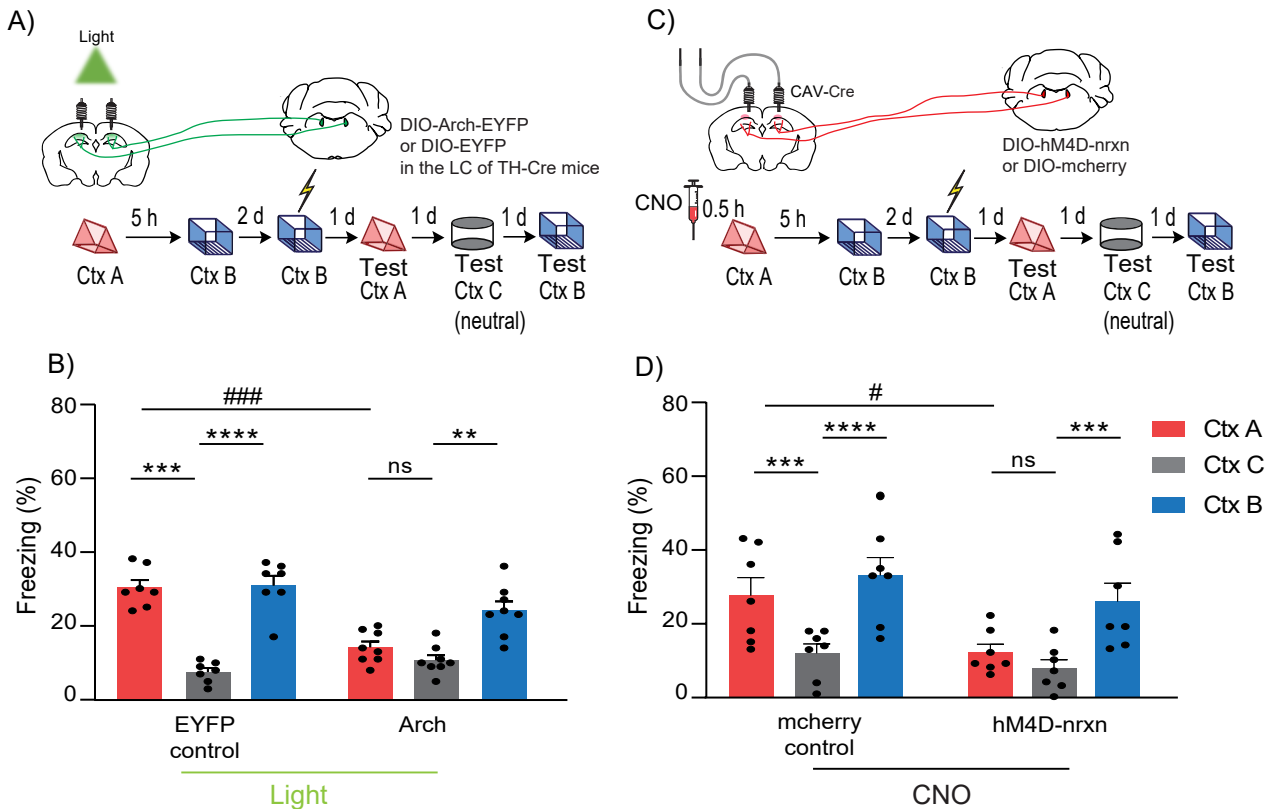
Suppl. Fig 4 (Related to Main Figure 1). Role of LC projections to dCA1 in contextual memory linking

A. Schematics of experimental design for surgery. In TH-Cre mice, DIO-Arch-EYFP (LC projections inhibited) or DIO-EYFP (control) was injected in LC. During exploration of context A, all the mice received bilateral green light (566 nm) through optic cannulas into dCA1 to inhibit the Arch (or EYFP controls) expressing LC fibers there.

B. Inhibition of LC fibers projecting to dCA1 during exploration of context A impaired contextual memory linking. (Control, n=7; LC projection inhibited, n=8. Two-way repeated measures ANOVA, Sidak post hoc. nsp> 0.05, **p<0.01, ###p <0.001, ***p<0.001, ****p<0.0001). Context A- Ctx A, Context B- Ctx B, Context C- Ctx C (neutral). Line (Light) used to depict that green light was given to all mice. * is used to depict significance within groups and # is used to show significance between groups for two-way RM ANOVA.

C. Schematics of experimental design for surgery. In WT mice, CAV-Cre was injected in dCA1 and DIO-hM4D-nrxn-mcherry (LC projections inhibited) or DIO-mcherry (control) was injected in LC. 30 min before exploration of context A, all the mice received bilateral CNO infusion through guide cannulas into dCA1 to locally inhibit synaptic-Gi (hM4D-nrxn) expressing LC fibers there during context A.

D. Inhibition of LC fibers projecting to dCA1 during exploration of context A impaired contextual memory linking. (Control, n=7; LC projection inhibited, n=7. Two-way repeated measures ANOVA, Sidak post hoc. nsp> 0.05, #p<0.05, **p<0.01, ***p<0.001, ****p<0.0001). Context A- Ctx A, Context B- Ctx B, Context C- Ctx C (neutral). Line (CNO) used to depict that CNO infusion was given to all mice. * is used to depict significance within groups and # is used to show significance between groups for two-way RM ANOVA.
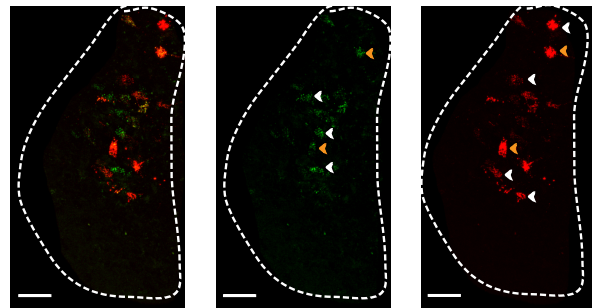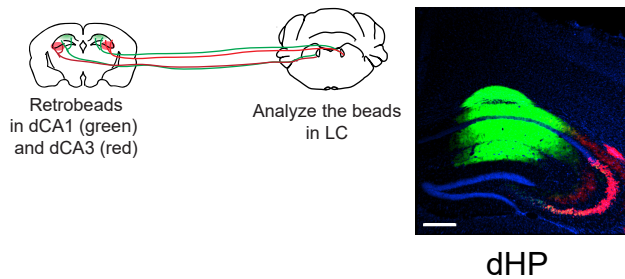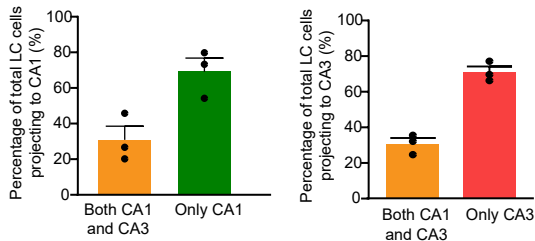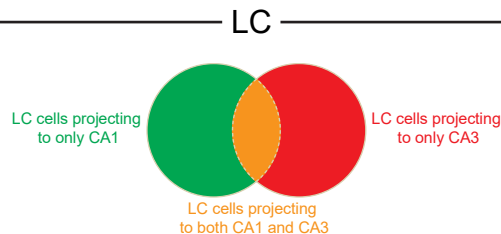
Suppl. Fig 5 (Related to Main Figures 1 and 2). Population of LC cells projecting to dCA1 and dCA3.

A. Schematics of experimental design for surgery. Green and red fluorescent retrobeads were injected in dCA1 and dCA3 respectively. Three weeks later, the mice were sacrificed to check for their expression in LC. Example images of HP and LC. Scale bar, 300 μm for HP and 40 μm for LC. The white arrows depict the single colored cells and the dark orange depict the dual-colored ones. The LC is outlined.

B. Percentage of LC cells projecting to dCA1 that also were projecting to dCA3 (i.e. expressing both green and red beads) out of the total LC cells projecting to dCA1 (i.e. expressing green beads) showed about 30.88 ± 7.67% were dCA3 projecting as well while 69.12 ± 7.67% were exclusive of dCA1. Similarly, out of the of the total LC cells projecting to dCA3 (i.e. expressing red beads), percentage of LC cells projecting to dCA1 as well (i.e. expressing both green and red beads) showed about 30.37 ± 3.17% were dCA1 projecting as well while 69.63 ± 3.17% were exclusive of dCA3. n=3 per group.

C. A diagrammatic representation of the overlapping population of the LC cells either projecting to dCA1 or dCA3 and both.
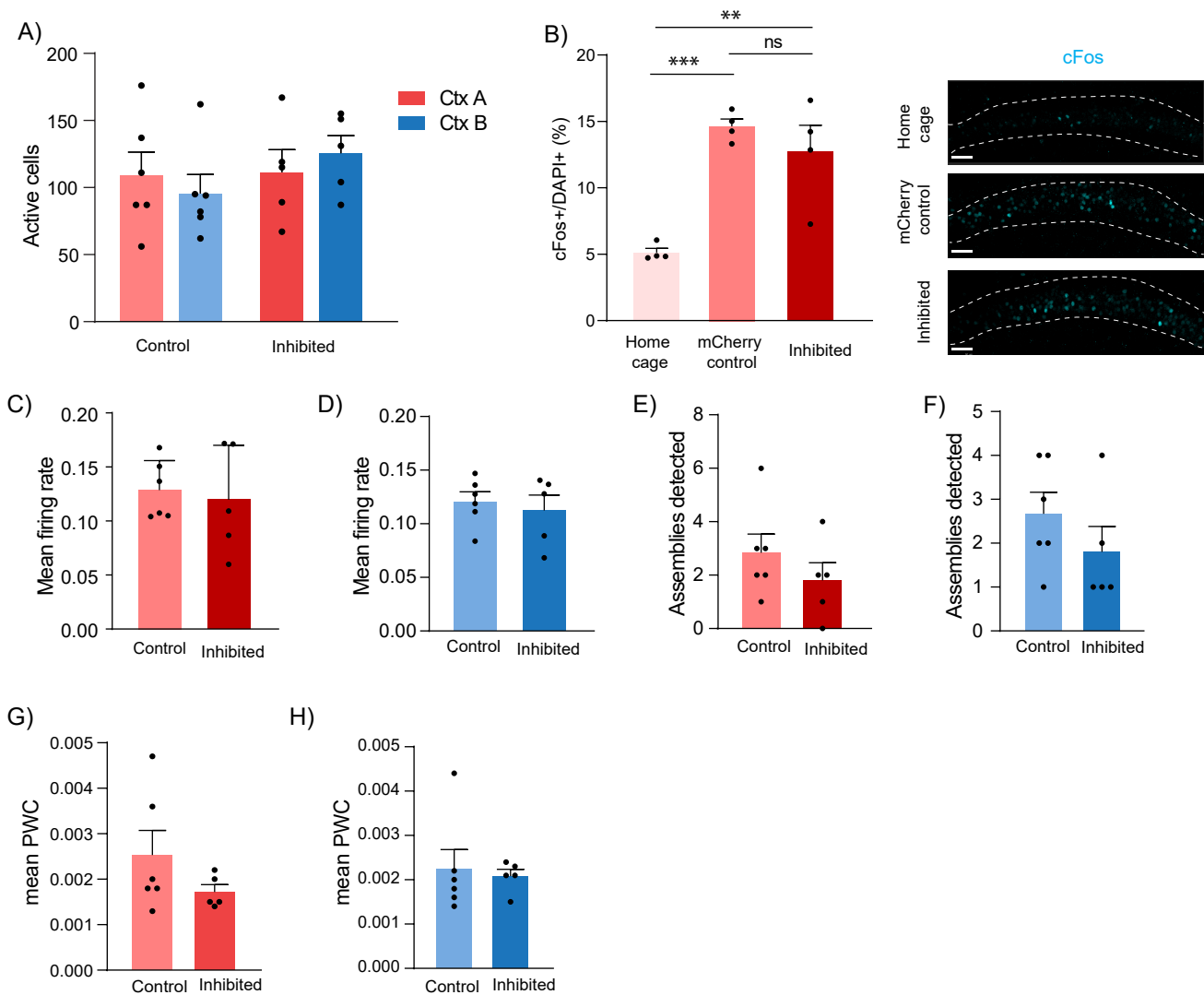
Suppl. Fig 6 (Related to Main Figure 4). Further analysis of calcium imaging data and cFos to show the effect of LC-dCA1 inhibition on neuronal ensembles.

A. Total number of active cells detected in dCA1 by calcium imaging does not change in either context upon inhibition of LC cells projecting to dCA1 during exploration of context A. Two-way RM ANOVA, Sidak posthoc.

B. Induction of cFos upon novel context exploration in dCA1 was not affected by inhibition of LC cells projecting to dCA1, n= 4 in all groups, One-way ANOVA, Fisher's LSD. Example images for cFos- cyan, principal layer of dCA1 outlined, scale bar, 50 μm.

C. There is no difference in mean firing rates in context A of the neurons active in both contexts A and B (overlapping neurons). Unpaired t-test.

D. There is no difference in mean firing rates in context B of the overlapping neurons. Unpaired t-test.

E. There is no difference in total assemblies of the overlapping neurons detected in context A. Unpaired t-test.

F. There is no difference in total assemblies of the overlapping neurons detected in context B. Unpaired t-test.

G. There is no difference in mean pair-wise correlation of the overlapping neurons detected in context A. Unpaired t-test.

H. There is no difference in mean pair-wise correlation of the overlapping neurons detected in context B. unpaired t-test. Control n=6, and LC inhibited n=5 for A, C-H.
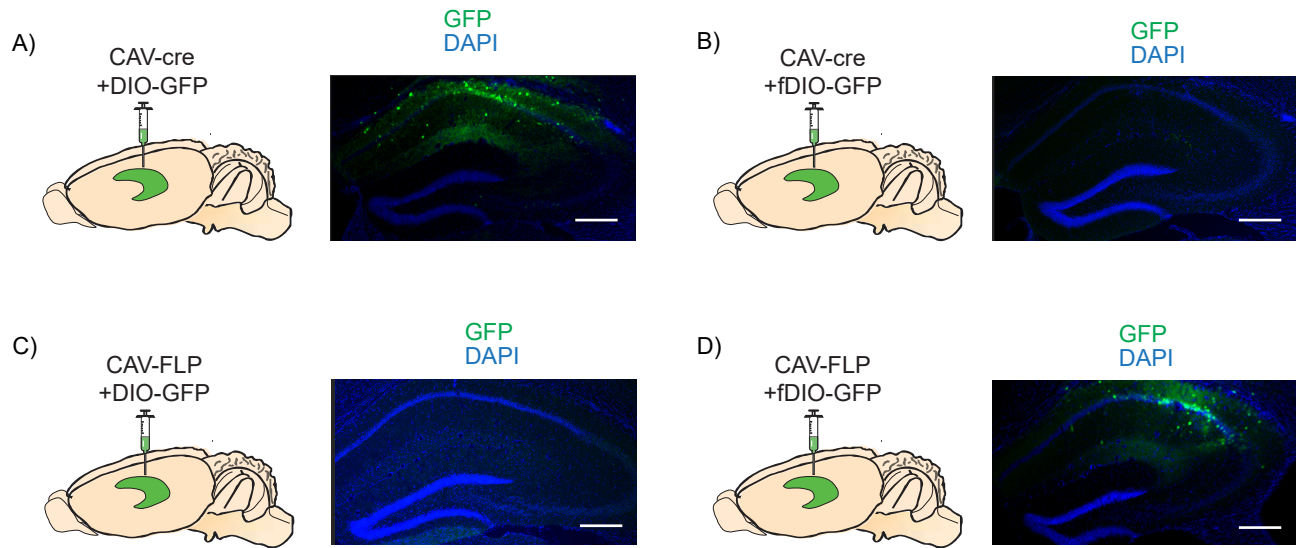
Suppl. Fig 7 (Related to Main Figure 7). Confirmation of non-interference between Cre-DIO and Flp-fDIO systems

A. Schematics of experimental design. A cocktail of CAV-cre and DIO-GFP was injected in dCA1. The expression of GFP shows the functionality of the cre-DIO system. GFP- green, DAPI- blue. Scale bar, 50μm.
B. Schematics of experimental design. A cocktail of CAV-cre and fDIO-GFP was injected in dCA1. The lack of expression of GFP confirms that the incompatibility of the two systems. GFP- green, DAPI- blue. Scale bar, 50μm.
C. Schematics of experimental design. A cocktail of CAV-FLP and DIO-GFP was injected in dCA1. The lack of expression of GFP shows confirm that the incompatibility of the two systems. GFP- green, DAPI- blue. Scale bar, 50μm.
D. Schematics of experimental design. A cocktail of CAV-FLP and fDIO-GFP was injected in dCA1. The expression of GFP shows the functionality of the FLP-fDIO system. GFP- green, DAPI- blue. Scale bar, 50μm.

Property	mcherry control	hM4Di (Gi)	P value	Statistical test
RMP (mV)	-70.1 $\pm$ 0.8	-71 $\pm$ 0.5	0.36	Unpaired t-test
Rin (MΩ)	159.7 $\pm$ 17.1	146.3 $\pm$ 17.1	0.55	Mann Whitney test
Rheobase (pA)	79 $\pm$ 7.2	101.7 $\pm$ 8	0.047*	Mann Whitney test
pAHP (mV)	-0.55 $\pm$ 0.1	-0.6 $\pm$ 0.2	0.87	Mann Whitney
AP threshold	-49.88 $\pm$ 0.45	-47.88 $\pm$ 0.95	0.07	Unpaired t-test

Suppl. Table 1: Passive membrane properties of dCA1 pyramidal neurons. There was no difference in the resting membrane potential (RMP), input resistance (Rin), peak afterhyperpolarization potential (pAHP) and action potential threshold (AP threshold) of neurons from mcherry control and hM4Di (Gi) mice. However, the rheobase current required to fire an action potential was significantly increased in dCA1 neurons of the hM4Di(Gi) group. Mean $\pm$ s.e.m.
Related to Main Figure 3

Property	GFP	Opto-D1	p	Statistical test
RMP (mV)	-69 $\pm$ 1.5	-66 $\pm$ 1.3	0.11	Mann Whitney test
Rin (MΩ)	180.8 $\pm$ 19.7	214.6 $\pm$ 21.7	0.26	Unpaired t-test
Rheobase (pA)	106.1 $\pm$ 19.3	95 $\pm$ 15.9	0.76	Mann Whitney test
pAHP	-1.5 $\pm$ 0.4	-0.45 $\pm$ 0.3	0.072	Mann Whitney test
AP threshold	-50.4 $\pm$ 2	-50.2 $\pm$ 1.5	0.5	Mann Whitey test

Suppl. Table 2: Passive membrane properties of dCA1 pyramidal neurons. There was no difference in the resting membrane potential (RMP), input resistance (Rin), rheobase (pA), peak afterhyperpolarization (pAHP) and threshold to fire action potentials (AP threshold) of neurons from GFP and opto-D1 activated mice. Mean $\pm$ s.e.m.
Related to Main Figure 7

Parameters of the microcircuit model		
N_{pyr}	Number of excitatory neurons	400
N_{inh}	Number of inhibitory neurons	50 dendrite-targeting (DT) 50 soma-targeting (ST)
N_{dend}	Number of dendritic subunits per neuron	20 for excitatory 1 for interneurons
$N_{pyr \to ST}$	Total number of synapses from excitatory neurons to soma-targeting(ST) interneurons	1000
$N_{pyr \to DT}$	Total number of synapses from excitatory neurons to dendrite-targeting (DT)	1000
$N_{ST \to pyr}$	Total number of synapses from ST interneurons to excitatory neurons	10000

$N_{DT \to pyr}$	Total number of synapses from DT interneurons to excitatory neurons	2000
$N_{input \to pyr}$	Total number of weak connections from input afferents to pyramidal dendrites per memory	5600
E_L	Leakage reversal potential	0 mV
g_E	Dendritic excitatory synaptic conductance	26 nS
g_I	Dendritic inhibitory synaptic conductance	20nS
g_{Ld}, g_L	Dendritic/somatic leak conductance	50nS
g_{Inh}	Somatic inhibitory current scaling constant	600nS
τ_{Inh}	Somatic inhibitory current time constant	30msec
E_E	Excitatory synapse reversal potential	+70mV
EI	Inhibitory synapse reversal potential	-10mV
C	Membrane capacitance	200pF
τ_{dend}	Dendritic membrane time constant	Inhibitory: 20msec Excitatory: 25msec
V_d	Dendritic Depolarization	-10mV <Vd< 70mV
g_{ax}	Axial conductance	30nS
θ_{soma}	Voltage threshold for somatic spikes	18mV
τ_{adapt}	Adaptation time constant of excitatory neurons	Baseline excitability: 200msec High excitability: 100msec
β_{adapt}	Adaptation reset constant for adaptation current I_{adapt}	Baseline Excitability: 2.8+0.45*I_{adapt} High Excitability: 1+ I_{adapt}
A_{adapt}	Adaptation coupling parameter	0.02
τ_{bAP}	Back propagating action potential time constant	10msec
E_{bAP}	Back propagating action potential max amplitude	5 mV
Θ_{PRP}	Calcium threshold for somatic Plasticity-Related Protein (PRP) synthesis	40.0
τ_{PRP}	Time constant for PRP decay	60 minutes
τ_H	Time constant of homeostatic synaptic scaling	720 hours

Suppl. Table 2: Parameters of the microcircuit model
Related to Main Figure 5